

# PCCP

Accepted Manuscript



This article can be cited before page numbers have been issued, to do this please use: M. M. Pereira, K. A. Kurnia, F. L. Sousa, N. J. O. Silva, J.A. Lopes-da-Silva, J. A.P. Coutinho and M. G. Freire, *Phys. Chem. Chem. Phys.*, 2015, DOI: 10.1039/C5CP05873B.



This is an *Accepted Manuscript*, which has been through the Royal Society of Chemistry peer review process and has been accepted for publication.

*Accepted Manuscripts* are published online shortly after acceptance, before technical editing, formatting and proof reading. Using this free service, authors can make their results available to the community, in citable form, before we publish the edited article. We will replace this *Accepted Manuscript* with the edited and formatted *Advance Article* as soon as it is available.

You can find more information about *Accepted Manuscripts* in the [Information for Authors](#).

Please note that technical editing may introduce minor changes to the text and/or graphics, which may alter content. The journal's standard [Terms & Conditions](#) and the [Ethical guidelines](#) still apply. In no event shall the Royal Society of Chemistry be held responsible for any errors or omissions in this *Accepted Manuscript* or any consequences arising from the use of any information it contains.

## ARTICLE

# Contact Angles and Wettability of Ionic Liquids on Polar and Non-polar Surfaces†

Cite this: DOI: 10.1039/x0xx00000x

Matheus M. Pereira<sup>a,†</sup>, Kiki A. Kurnia<sup>a,b,†</sup>, Filipa L. Sousa<sup>a</sup>, Nuno J. O. Silva<sup>c</sup>, José A. Lopes-da-Silva<sup>d</sup>, João A. P. Coutinho<sup>a</sup>, and Mara G. Freire<sup>a,\*</sup>Received 00th January 2012,  
Accepted 00th January 2012

DOI: 10.1039/x0xx00000x

[www.rsc.org/](http://www.rsc.org/)

Many applications involving ionic liquids (ILs) require the knowledge of their interfacial behaviour, such as wettability and adhesion. In this context, herein, two approaches were combined aiming at understanding the impact of the IL chemical structures toward their wettability in both polar and non-polar surfaces, namely: (i) the experimental determination of the contact angles of a broad range of ILs (covering a wide number of anions of variable polarity, cations, and cation alkyl side chain lengths) in polar and non-polar solid substrates (glass, Al-plate, and poly-(tetrafluoroethylene) (PTFE)); and (ii) the correlation of the experimental contact angles with the cation-anion pair interaction energies generated by the Conductor-like Screening Model for Real Solvents (COSMO-RS). The combined results reveal that the ILs hydrogen-bond basicity, and thus the IL anion, plays a major role through their wettability in both polar and non-polar surfaces. The increase of the IL hydrogen-bond accepting ability leads to an improved wettability of more polar surfaces (lower contact angles) while the opposite trend is observed in non-polar surfaces. The cation nature and alkyl side chain lengths have however a smaller impact through the ILs wetting ability. Linear correlations were found between the experimental contact angles and the cation-anion hydrogen-bonding and cation ring energies, estimated using COSMO-RS, suggesting that these features primarily control the wetting ability of ILs. Furthermore, two-descriptor correlations are here proposed to predict the contact angles of a wide variety of ILs in glass, Al-plate, and PTFE surfaces. A new extended list is provided for the contact angles of ILs in three surfaces, which can be used as *a priori* information to choose appropriate ILs before a given application.

## Introduction

In recent decades, ionic liquids (ILs) have attracted significant attention as neoteric solvents for chemical reactions and separation processes due to their remarkable properties, such as non-volatility, negligible vapour pressure, and high thermal and chemical stabilities.<sup>1</sup> Nonetheless, the most fascinating feature arises from the possibility of tuning their physicochemical properties by simply varying their constituting ions,<sup>2</sup> so that an IL with desirable properties can be designed for a specific application. As a result, ILs have been studied as alternative media for numerous applications.<sup>3-5</sup> For applications involving ILs in heterogeneous systems and transport in capillary, fibrous, or porous environments, their interfacial properties, such as surface/interfacial tension and wettability (the tendency of a fluid to spread on a given solid surface that may be estimated by the measurement of the contact angle), have to be known. Although some attention has been devoted to the surface tension of pure ILs and their mixtures with molecular solvents,<sup>6</sup> the determination of contact angles of ILs in solid surfaces, aiming at characterizing their wettability, has received a limited

attention.<sup>7-13</sup> Gao and McCarthy<sup>8</sup> reported the wettability of four ILs on various hydrophobic and super-hydrophobic surfaces, and highlighted a significant complex analysis of the ILs contact angles since both ions of the probe liquid can interact with the surfaces evaluated. Restolho et al.<sup>9-12</sup> and Carrera et al.<sup>13</sup> described the wetting behaviour of ILs as a main result of their dispersive and non-dispersive interactions with the solid substrate. Other researchers<sup>14-18</sup> turned to electrowetting studies aiming at enhancing wettability by applying an external voltage across the solid-liquid interface. While all these works<sup>7-18</sup> contribute to the understanding of the wetting phenomenon, there are still few ILs investigated and the lack of a comprehensive analysis of the impact of the ILs chemical structures and their wetting behaviour.

A fundamental understanding of the relationship between the ILs chemical structures and wettability is of crucial relevance envisaging a rational synthesis and design of ILs for a specific task, particularly when taking into consideration the large number of possible ILs that can be synthesized. The

studies being carried out by us have been focused on combining experimental and theoretical or computational-based approaches aiming at identifying promising ILs candidates for specific purposes before carrying out extensive and trial-and-error experimental measurements. In previous works, we have established the connection between the ILs chemical structures and their mutual solubilities with water.<sup>19-27</sup> More recently, we have correlated the hydrogen-bond acceptor and donor abilities of ILs with the IL cation-anion interaction energies, allowing us to propose extended basicity<sup>28</sup> and acidity<sup>29</sup> scales for ILs. Furthermore, based on computational approaches, we have designed and proposed three potential novel ILs to be used as absorbents in absorption-refrigeration systems,<sup>30</sup> and have also identified promising ILs for the desulfurization of fuels,<sup>31</sup> and for the extraction of ethanol in IL-water mixtures.<sup>32</sup> These works show how the fundamental knowledge on structure-property relationships of ILs allow their adequate design to meet the requirements of a target application.

Herein, aiming at understanding the impact of the ILs chemical structures on their wetting ability in both polar and non-polar surfaces, the contact angles of a broad range of ILs, comprising a wide selection of cations, anions and cation alkyl side chain lengths, were experimentally determined. The novel experimental data for a large variety of ILs was then interpreted and discussed taking into account their chemical structures. The contact angle data were subsequently correlated with the interaction energies of the IL cation-anion pairs generated by the Conductor-like Screening Model for Real Solvent (COSMO-RS).<sup>33,34</sup> Based on their linear dependence, an extended list for the wettability of 480 ILs in 3 surfaces is here proposed.

## Results and Discussion

### Contact Angle Measurements

The experimental contact angle values at 298.2 K for the ILs investigated in this work are reported in Table 1. A comparison with literature data is challenging due to lack of values for the same surfaces. Nevertheless, a good agreement is observed between the data measured in this work and those previously published by Carrera et al.<sup>13</sup> In particular, the contact angles of [C<sub>4</sub>C<sub>1</sub>im][NTf<sub>2</sub>] ( $\theta = 66.25^\circ$ )<sup>13</sup> and [C<sub>4</sub>C<sub>1</sub>im][N(CN)<sub>2</sub>] ( $\theta = 81.71^\circ$ )<sup>13</sup> on PTFE are in close agreement with the values obtained in this work. On the other hand, the same authors<sup>13</sup> reported a much higher contact angle of [C<sub>4</sub>C<sub>1</sub>im][BF<sub>4</sub>] ( $\theta = 81.71^\circ$ ) on PTFE than the value here measured (65.07°). Batchelor et al.<sup>35</sup> and Restolho et al.<sup>9</sup> also reported the contact angle of [C<sub>4</sub>C<sub>1</sub>im][BF<sub>4</sub>] on the same surface, and their values were 79° and 95°, respectively. This disagreement in contact angle values could be a result of the different IL samples used and their respective purity level and/or water content. Indeed, Freire et al.<sup>36</sup> have demonstrated that [C<sub>4</sub>C<sub>1</sub>im][BF<sub>4</sub>], in the presence of water, is not stable and has high tendency to suffer hydrolysis. Therefore, the chemical stability of [C<sub>4</sub>C<sub>1</sub>im][BF<sub>4</sub>] (either in our samples or those used by other authors) should be

behind the differences reported. Even so, given the fluorinated nature of the IL anion and of the PTFE surface, low contact angles are expected for [C<sub>4</sub>C<sub>1</sub>im][BF<sub>4</sub>].

Table 1. Contact angles,  $\theta$ , of the ILs investigated on the polar glass and Al-plate surfaces, and on the non-polar PTFE surface, at 298.2 K, along with the respective standard deviations,  $\sigma$ .

Ionic Liquids	$(\theta \pm \sigma)/\text{deg}$		
	Glass	Al-plate	PTFE
[C <sub>4</sub> C <sub>1</sub> im][Ac]	20.63 ± 0.03	17.67 ± 0.01	98.03 ± 0.02
[C <sub>4</sub> C <sub>1</sub> im][DMP]	24.56 ± 0.91	25.64 ± 0.17	90.48 ± 0.16
[C <sub>4</sub> C <sub>1</sub> im][TFA]	31.03 ± 0.11	32.79 ± 0.05	83.43 ± 0.36
[C <sub>4</sub> C <sub>1</sub> im][N(CN) <sub>2</sub> ]	32.54 ± 0.99	34.60 ± 0.02	82.38 ± 0.30
[C <sub>4</sub> C <sub>1</sub> im][EtSO <sub>4</sub> ]	33.25 ± 0.94	35.36 ± 0.17	80.32 ± 0.32
[C <sub>4</sub> C <sub>1</sub> im][MeSO <sub>4</sub> ]	36.11 ± 0.70	35.57 ± 0.02	79.54 ± 0.26
[C <sub>4</sub> C <sub>1</sub> im][CF <sub>3</sub> SO <sub>3</sub> ]	37.24 ± 0.11	43.45 ± 0.88	76.43 ± 0.17
[C <sub>4</sub> C <sub>1</sub> im][SCN]	39.21 ± 0.91	44.75 ± 0.27	74.77 ± 0.19
[C <sub>4</sub> C <sub>1</sub> im][C(CN) <sub>3</sub> ]	39.57 ± 0.40	44.91 ± 0.68	72.74 ± 0.06
[C <sub>4</sub> C <sub>1</sub> im][NTf <sub>2</sub> ]	43.87 ± 0.12	49.43 ± 0.43	66.76 ± 0.06
[C <sub>4</sub> C <sub>1</sub> im][BF <sub>4</sub> ]	45.63 ± 0.50	52.13 ± 0.10	65.07 ± 0.07
[C <sub>4</sub> C <sub>1</sub> im][PF <sub>6</sub> ]	52.46 ± 0.93	57.20 ± 0.27	60.11 ± 0.07
[C <sub>2</sub> C <sub>1</sub> im][NTf <sub>2</sub> ]	37.66 ± 0.35	48.50 ± 0.21	66.93 ± 0.01
[C <sub>3</sub> C <sub>1</sub> im][NTf <sub>2</sub> ]	42.85 ± 0.05	49.01 ± 0.09	66.82 ± 0.06
[C <sub>5</sub> C <sub>1</sub> im][NTf <sub>2</sub> ]	43.96 ± 0.23	50.29 ± 0.36	66.53 ± 0.03
[C <sub>6</sub> C <sub>1</sub> im][NTf <sub>2</sub> ]	44.12 ± 0.10	51.22 ± 0.11	66.10 ± 0.38
[C <sub>7</sub> C <sub>1</sub> im][NTf <sub>2</sub> ]	45.09 ± 0.14	52.07 ± 0.02	65.95 ± 0.15
[C <sub>8</sub> C <sub>1</sub> im][NTf <sub>2</sub> ]	48.58 ± 0.23	52.60 ± 0.13	65.60 ± 0.17
[C <sub>9</sub> C <sub>1</sub> im][NTf <sub>2</sub> ]	46.11 ± 0.69	53.28 ± 0.52	64.14 ± 0.33
[C <sub>3</sub> C <sub>1</sub> pip][NTf <sub>2</sub> ]	37.02 ± 0.17	48.99 ± 0.63	71.97 ± 0.78
[C <sub>4</sub> C <sub>1</sub> pip][NTf <sub>2</sub> ]	41.99 ± 0.13	49.30 ± 0.27	67.21 ± 0.02
[C <sub>4</sub> -4-C <sub>1</sub> py][NTf <sub>2</sub> ]	41.04 ± 0.07	49.26 ± 0.16	68.88 ± 0.80

The data presented in Table 1 show that, for the same IL, the contact angles on the glass and Al-plate surfaces are lower than on PTFE, and follow the trend: glass < Al-plate < PTFE. In general, the glass and Al-plate surfaces are easier to wet by more hydrophilic ILs or with a higher hydrogen-bond basicity, such as [C<sub>4</sub>C<sub>1</sub>im][Ac] and [C<sub>4</sub>C<sub>1</sub>im][DMP].<sup>28</sup> In the glass surface, the presence of surface hydroxyl groups should be responsible for the improved wetting behaviour. Using molecular dynamics simulations, Cione et al.<sup>37</sup> have shown that the interactions between the -OH groups on the glass surface and the IL ions decreases the strength of the cation-anion interactions, further inducing a decrease in the local surface tension and, consequently, improves the ILs wetting ability. On the other hand, higher contact angle values were observed for the PTFE surface, and that can be attributed to the chemical structure/nature of the organofluoride polymer. Even so, ILs

with fluorinated anions display lower contact angles on the PTFE surface than those composed of non-fluorinated anions. In this polymer, the carbon atoms are linked to electronegative and repulsive fluorine atoms minimizing thus the interactions of ILs with PTFE.<sup>38</sup> These results reveal significant wettability differences of ILs in polar and non-polar surfaces where, on the whole, ILs have a higher affinity to wet polar surfaces – a direct outcome of their remarkable hydrogen-bonding ability as discussed below.

The wide range of ILs studied in this work allows investigating the impact of the structural variations of ILs, namely the anion and cation nature, as well as the cation alkyl side chain length, on their wetting ability of polar and non-polar surfaces. By changing the IL anion, the contact angle values vary significantly on glass surfaces - from 20.63° for [C<sub>4</sub>C<sub>1</sub>im][Ac] to 52.46° for [C<sub>4</sub>C<sub>1</sub>im][PF<sub>6</sub>]. The glass surface is easier to wet by the polar [C<sub>4</sub>C<sub>1</sub>im][Ac] rather than using the more hydrophobic [C<sub>4</sub>C<sub>1</sub>im][PF<sub>6</sub>]. For [C<sub>4</sub>C<sub>1</sub>im]-based ILs, anions can be ranked based on increasing contact angles in the glass surface as follows: [Ac]<sup>-</sup> < [DMP]<sup>-</sup> < [TFA]<sup>-</sup> < [N(CN)<sub>2</sub>]<sup>-</sup> < [EtSO<sub>4</sub>]<sup>-</sup> < [MeSO<sub>4</sub>]<sup>-</sup> < [CF<sub>3</sub>SO<sub>3</sub>]<sup>-</sup> < [SCN]<sup>-</sup> < [C(CN)<sub>3</sub>]<sup>-</sup> < [NTf<sub>2</sub>]<sup>-</sup> < [BF<sub>4</sub>]<sup>-</sup> < [PF<sub>6</sub>]<sup>-</sup>. This rank of anions closely follows the extended basicity scale of [C<sub>4</sub>C<sub>1</sub>im]-based ILs proposed by Cláudio et al.<sup>28</sup> Generally, the higher the anion hydrogen-bond basicity, *i.e.*, the ability of the IL anion to accept protons, the easier it is for the IL to wet the polar glass surface. A similar rank of anions to wet the polar Al-plate surface was observed (and in a slightly more expanded range of contact angle values). This phenomenon might be linked to the chemical structure of the aluminium plate surface. Anwender et al.<sup>39</sup> suggested the presence of surface coordination of aluminium atoms in monomeric or oligomeric forms, in particular the presence of highly acidic and reactive tri-coordinated Al(III) species. This “acidic” Al-plate surface has a high affinity toward ILs with high basicity and, ultimately, the surface is easier to wet using ILs of higher hydrogen-bond basicity. In summary, for polar glass and Al-plate surfaces, the hydrogen bonding ability of the anion plays a dominant role towards the ILs wetting ability – the higher the ILs hydrogen-bond basicity the easier is to wet the polar surfaces.

On the other hand, a reverse rank of the anions to wet the non-polar PTFE surface was observed; an increase in the IL hydrogen-bond basicity leads to higher contact angles, and thus to a decreased ability to wet this surface. The same anion trend was observed by Carrera et al.<sup>13</sup> While these authors<sup>13</sup> studied a more limited number of ILs, they showed the higher aptitude of low basicity ILs, such as [C<sub>4</sub>C<sub>1</sub>im][NTf<sub>2</sub>], to wet the non-polar PTFE surface when compared to ILs with higher basicity, *e.g.*, [C<sub>4</sub>C<sub>1</sub>im][N(CN)<sub>2</sub>]. In addition, the same rank of anions to wet the non-polar PTFE surface was also observed when some of these anions are combined with other cations, namely methyltrioctylammonium.<sup>13</sup> Li and co-workers,<sup>40</sup> using 6 ILs, also revealed that ILs with lower hydrogen-bond basicity have a higher ability to wet the non-polar PTFE surface.

Based on the results here obtained for an extended number of [C<sub>4</sub>C<sub>1</sub>im]-based ILs, and other literature values previously

reported,<sup>13,40</sup> it is clear that the hydrogen-bond basicity of the IL anion plays a dominant role on the ILs wettability, either in polar or non-polar surfaces. In polar surfaces the ILs wettability increases with their hydrogen-bond basicity, whereas the opposite effect is observed for non-polar surfaces.

While the contact angle values significantly differ with the IL anion, the same was not observed with the IL cation head group and alkyl side chain length. For instance, increasing the alkyl side chain length from [C<sub>2</sub>C<sub>1</sub>im][NTf<sub>2</sub>] to [C<sub>9</sub>C<sub>1</sub>im][NTf<sub>2</sub>] results on a small increase of the contact angle on the glass surface, from 37.66° to 46.11°. A similar trend was observed with the Al-plate surface. Cations with short alkyl side chains are slightly more suitable to wet polar surfaces, as expected, owing to the higher hydrophobicity as the size of the alkyl chain increases. As observed previously with the IL anion effect, a reversed trend on the wettability is observed for the non-polar PTFE surface. Furthermore, for ILs with the same anion and longer alkyl side chains, the contact angle values become increasingly more similar amongst the several surfaces since the hydrogen-bonding interactions become less significant.

The results reported in Table 1 indicate that the IL anion plays the primary role on their wetting capacity, being thus a consequence of their hydrogen-bonding ability and to interact with each polar and non-polar surface, whereas the cation alkyl side chain length and the cation head group display a less significant and secondary effect. Nevertheless, it should be highlighted that they can be also used to adjust the wetting ability of ILs although in a narrower extent.

### COSMO-RS

Aiming at gathering a deeper insight into the mechanisms that control the wettability of ILs on polar and non-polar surfaces, as well as to attempt the development of a predictive model able to estimate *a priori* contact angle values that would help in the design of new ILs, COSMO-RS was used herein.

From COSMO-RS calculations, three cation-anion interaction energies, namely electrostatic/misfit,  $E_{MF}$ , hydrogen-bonding,  $E_{HB}$ , and van der Waals forces,  $E_{vdW}$ , can be estimated (plus the total interaction energy,  $E_{INT}$ ). These energy descriptors generated by COSMO-RS have been successfully used to describe the hydrogen-bond basicity<sup>28</sup> and acidity<sup>29</sup> of ILs, as well as the adsorption ability of ILs and chlorinated compounds onto carbon surfaces.<sup>41-43</sup> In addition to those descriptors, here we introduced an additional descriptor, the ring correction energy,  $E_{Ring}$ . The  $E_{INT}$ ,  $E_{MF}$ ,  $E_{HB}$ ,  $E_{vdW}$ , and  $E_{Ring}$  values for the studied ILs are given in Table S1 in the ESI†. These five descriptors allowed us to develop a model to predict IL contact angles on both polar and non-polar surfaces.

In order to select proper descriptors able to describe ILs contact angles on the different surfaces, a stepwise regression method was used. In this way, a stepwise model-building approach was addressed, starting with a single descriptor variable for the identification of an initial model. Then, the model was repeatedly improved from the previous step by adding (forward stepwise) or removing (back stepwise) a new

variable, while the stepwise approach stopped when no further improvements on the model were observed. The best single predictor for each correlation, initially selected according to the highest correlation coefficient obtained, was used for the initial linear regression step. As a next step, one descriptor was added at a time, always adding the one that improves the description, until no longer significant improvements were observed. The final regression equation was achieved when the significant variables were identified.

As an initial step to develop a correlation between the ILs wettability on the glass surface, as well as to infer on their possible dependence with cation-anion interaction energies, we correlated the experimental contact angles values acquired in this work as function of individual descriptors. The accuracy of the correlations was ascertained by the correlation coefficient,  $R^2$ , the Fisher significance parameter (a statistical significance test used in the analysis of contingency tables),  $F$ , and the average absolute relative deviation (AARD). The AARD was calculated using the equation given in the ESI†. The correlations that describe the one-descriptor models for the contact angles of ILs on the glass surface are given by Equation 1 in Table 2 (and Equations S1 to S4 in Table S2 in the ESI†) along with their statistical parameters. The one-descriptor parameter equations, using only  $E_{\text{INT}}$ ,  $E_{\text{MF}}$ ,  $E_{\text{vdW}}$ , or  $E_{\text{Ring}}$ , yield poor  $R^2$  and  $F$ , and high AARD values, and thus these are not statistically relevant in the description of the contact angles of ILs onto the glass surface. Additional information on these equations can be found in Table S2 in the ESI†. In summary, electrostatic and dispersive interactions have no significant impact on the contact angle, and consequently, on the wetting ability of ILs on polar glass surfaces. The correlation using  $E_{\text{HB}}$  produced the highest  $R^2$  and  $F$ , and lower AARD values when compared to the other one-descriptor correlations. This is a clear indication that the cation-anion hydrogen-bond energies of ILs reflects the hydrogen-bonding ability of their ions to interact with the glass surface, and thus, on their wetting ability. In this way, ILs with higher cation-anion interaction energies show an improved ability to wet the polar glass surface. This is in agreement with the contact angle dependence of the ILs hydrogen-bonding basicity discussed before. Thus, it can be

concluded that, among the three specific cation-anion interaction energies, hydrogen-bond plays a dominant role on their wettability aptitude onto polar surfaces.

Although a reasonable one-descriptor correlation using  $E_{\text{HB}}$  can be proposed for the glass surface, this model only yields a  $R^2$  of 0.8005 and  $F$  value of 101.2942 (cf. Equation 1 in Table 2). As such, even though Equation 1 might be useful for predicting the contact angles of ILs with similar chemical structures to those used in the dataset, higher  $R^2$  and  $F$  values are expected aiming at gathering more detailed molecular-level information on the wetting behaviour of ILs as well as to display some predictive ability for other ILs not used in the correlation development. For that purpose, the correlation of the measured contact angles using a multi-descriptor approach was attempted. Since the  $E_{\text{HB}}$  was found to play the dominant role, extra descriptors were further added to Equation 1 resulting in a series of Equations listed in Table 2 (and Equations S5-S10 in Table S2 in the ESI†). It should be noted that  $E_{\text{INT}}$  is not included in the development of multi-descriptor correlations as it does not represent any specific type of interaction. Adding  $E_{\text{MF}}$  or  $E_{\text{vdW}}$  to Equation 1 leads to correlations with similar  $R^2$  and  $F$  values (cf. Equation S5 and S6 in Table S2 in the ESI†) and thus, these two-descriptor correlations are not statistically significant. Curiously, the combination of  $E_{\text{MF}}$  and  $E_{\text{vdW}}$  (cf. Equation S7 in Table S2 in the ESI†) gives a correlation with  $R^2$  and  $F$  values lower than Equation 1 and, therefore, further confirming that electrostatic/misfit interactions and van der Waals forces do not have a significant contribution towards the wetting ability of ILs. Significant improvements on the  $R^2$  and  $F$  values, 0.9117 and 130.1319, respectively, can be achieved by combining  $E_{\text{HB}}$  and  $E_{\text{Ring}}$  (cf. Equation 2 in Table 2) which is an indication that the contact angles of ILs on polar glass surfaces is not only controlled by hydrogen-bonding interactions, but also by the ring energy, which depends on the number of atoms forming the ring, and thus on the IL size and steric effects. Nevertheless, it should be taking into account that the presence of cyclic cations can also influence the cation-anion cohesive energy and further ability of the IL anion to interact with each surface.

Table 2. Correlation between the experimental contact angles of ILs on the polar SiO<sub>2</sub> (glass),  $\theta_{\text{G}}$ , Al-plate,  $\theta_{\text{Al}}$ , and non-polar PTFE (Teflon),  $\theta_{\text{T}}$ , surfaces and the cation-anion interaction energies (in kJ·mol<sup>-1</sup>) estimated using COSMO-RS. The respective correlation coefficient,  $R^2$ , Fisher significance parameter,  $F$ , and average absolute standard deviation, AARD, are also provided.

	$R^2$	$F$	AARD/%	Equation
$\theta_{\text{G}} = ((0.7346 \pm 0.0730) \times E_{\text{HB}}) + (49.95 \pm 1.17)$	0.8005	101.2942	5.29	(1)
$\theta_{\text{G}} = ((0.8336 \pm 0.0516) \times E_{\text{HB}}) + ((10.02 \pm 1.79) \times E_{\text{Ring}}) + (91.38 \pm 7.45)$	0.9117	130.1319	3.89	(2)
$\theta_{\text{Al}} = ((1.0414 \pm 0.0554) \times E_{\text{HB}}) + (59.45 \pm 0.88)$	0.9338	353.8392	3.91	(3)
$\theta_{\text{Al}} = ((1.1201 \pm 0.0365) \times E_{\text{HB}}) + ((7.96 \pm 1.26) \times E_{\text{Ring}}) + (92.39 \pm 5.25)$	0.9746	481.8869	3.08	(4)
$\theta_{\text{T}} = ((-0.9855 \pm 0.0606) \times E_{\text{HB}}) + (58.45 \pm 0.96)$	0.9133	264.4063	2.68	(5)
$\theta_{\text{T}} = ((-1.0788 \pm 0.0333) \times E_{\text{HB}}) + ((-9.45 \pm 1.15) \times E_{\text{Ring}}) + (19.35 \pm 4.80)$	0.9769	481.8869	3.08	(6)

The same type of approach was applied for the correlation of the contact angles of ILs on the Al-plate surface (cf. Equations 3 and 4 in Table 2, and Equations S11-S20 in Table S3 in the ESI†). Similar trends were observed, in which an

evaluation of the best models identifies the hydrogen-bond interaction energy descriptor,  $E_{\text{HB}}$ , as the most statistically significant. Even so, the one-descriptor model using  $E_{\text{HB}}$  to correlate the contact angles on the polar Al-plate produces

higher  $R^2$  and  $F$  values (*cf.* Equation 3 in Table 2) than on the glass surface. This observation may indicate that the hydrogen-bonding of the ILs ions with the Al-surface is more relevant than that observed in the glass surface where the size of the cation ring also played a role. However, the  $E_{\text{Ring}}$  also has a secondary influence on the wetting behaviour of ILs onto the Al-plate since higher  $R^2$  and  $F$  values were obtained when including this descriptor.

A similar procedure was applied for the correlation of the contact angles of ILs in the PTFE surface. Unlike glass and Al-plate, the PTFE surface is non-polar. Nevertheless, the correlations obtained (*cf.* Equations 5 and 6, and Equations S21-S30 in Table S4 in the ESI†) reveal that the hydrogen-bonding interactions of the cation-anion pairs also play the dominant role toward the contact angle, and subsequently, on the wetting ability of ILs on the non-polar PTFE surface, albeit in an opposite trend to that observed with the polar surfaces (as denoted by the negative values of the coefficients in the equations corresponding to PTFE). The stronger the hydrogen-bond strength of the IL ions pairs, the lower their interaction with the PTFE surface (supported by high contact angle values). Similar to the correlations obtained for the polar surfaces, the two-descriptor correlations which contain hydrogen-bonding and cation ring size energies, prove to be the most statistically significant.

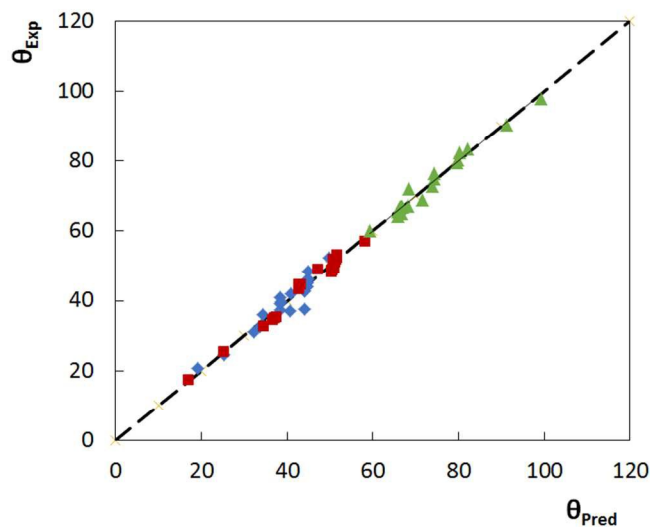


**Figure 1.** Comparison between experimental (at 298.2 K) and predicted contact angle of ILs on polar and non-polar surfaces. Symbols: (♦), Glass; (■), Al-plate; and (▲), PTFE.

In summary, the contact angles of a large number of ILs on polar and non-polar surfaces can be described by a fixed set of quantum-derived parameters, namely by IL cation-anion interaction energies. Equations 2, 4, and 6 were then used to estimate the  $\theta$  values of neat ILs (the comparison using other equations is given in Figures S1-S30 in the ESI†). Figure 1 depicts the relationship between the experimental and estimated  $\theta$  parameters. There is a close agreement between the

experimental and predicted  $\theta$  meaning that Equations 2, 4, and 6 can thus be used to predict the contact angles of a wide variety of ILs with reasonable accuracy. These three equations were constructed using a broad range of chemically different ILs, comprising imidazolium-, piperidinium-, and pyridinium cations, anions of almost extreme hydrogen-bond basicity ( $[\text{C}_4\text{C}_1\text{im}][\text{DMP}] = 1.12$  versus  $[\text{C}_4\text{C}_1\text{im}][\text{PF}_6] = 0.21$ )<sup>28,44</sup>, and with cations with variable alkyl side chains length. Correlations with high  $R^2$  and  $F$  values were obtained further validating the use of the *a priori* cation-anion interaction energy descriptors for the prediction of the contact angles of ILs on both polar glass and Al-plate and in the non-polar PTFE surfaces.

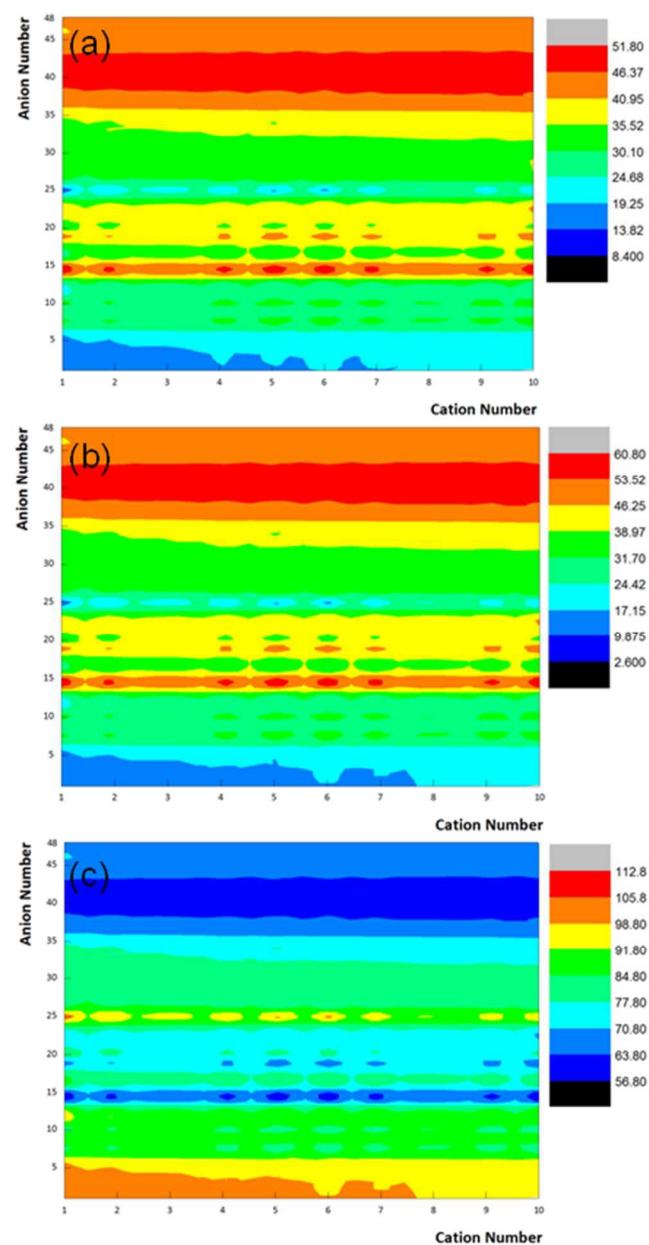


**Figure 2.** Predicted contact angles of 480 ILs on glass (a), Al-plate (b) and PTFE (c) surfaces.

In recent years, a significant progress has been made in identifying structure-related descriptors aiming at describing the physicochemical properties of ILs, such as density,<sup>45</sup> polarity,<sup>46</sup> basicity/acidity,<sup>28</sup> and toxicity.<sup>47</sup> However, there still lacks a databank or predictive methods for the contact angles of ILs on both polar and non-polar surfaces. Driven by the prediction results presented above, Equations 2, 4, and 6 were then used to predict the contact angles of other ILs not studied in this work (or ILs with no experimental data yet available). A database of contact angles of ILs on polar and non-polar surfaces comprising 10 1-alkyl-3-methylimidazolium-based cations (this set of cations was chosen because these are the most studied ILs so far) combined with 48 anions of different hydrogen-bond basicity, resulting in a total of 480 ILs, was finally built. This novel data set contains ILs with similar structures in the database, such as ILs with propanoate ([Pro]<sup>-</sup>), butanoate ([But]<sup>-</sup>) and hexanoate ([Hex]<sup>-</sup>) which have similar structures to [Ac]<sup>-</sup> and that is used in the training dataset. For other ILs, none or similar anions are present in the experimental data set, such as tris(pentafluoroethyl)trifluorophosphate, [eFAP]<sup>-</sup>; and tris(nonafluorobutyl)trifluorophosphate, [bFAP]<sup>-</sup>. In general, the extent of this database can be as large as desired since the correlation methods developed only require cation-anion interaction energies that can be estimated using COSMO-RS. The full name, abbreviation, and cation or anion numbering of ILs, along with their cation-anion interaction energy descriptors, are given in Table S5 in the ESI†. The predicted  $\theta$  values on polar and non-polar surfaces are given in Table S6 in the ESI† and depicted in Figure 2.

In general, ILs composed of hydrogensulphate or carboxylate-based anions (anions number 1 to 6, for full anion number see Table S5 in the ESI†), display low contact angles regardless of the cation alkyl chain length. On the opposite, these ILs display high contact angles on the non-polar PTFE surface. It is also noteworthy to mention that ILs with a low hydrogen-bond basicity anion, such as [eFAP]<sup>-</sup> and [bFAP]<sup>-</sup>, show high contact angles on the glass and Al-plate surfaces, while presenting low contact angles on the PTFE surface. The predicted contact angles reinforce the idea that while the IL anion has significant influence on their wetting ability, the cation core and alkyl chain length only present a slightly contribution. For instance, the predicted contact angles in the glass surface just varied from 17.18° to 19.91° for [C<sub>1</sub>C<sub>1</sub>im][Ac] to [C<sub>10</sub>C<sub>1</sub>im][Ac]. These structural variations may, however, be used to fine-tune the physical properties of ILs to meet the requirement of a task-specific application. In summary, Figure 2 depicts the prediction of the contact angles of 480 ILs in 3 surfaces that can be used as *a priori* information before extensive and experimental trial-and-error approaches.

## Conclusions

In this work, a comprehensive investigation on the impact of the chemical structures of ILs (cation head group, anion nature, and cation alkyl side chain length) on their wettability of polar and non-polar surfaces was carried out through the

experimental measurements of contact angles. The gathered results, at least considering the families of ILs investigated in this work, demonstrate that the ions hydrogen-bonding ability plays a dominant role – the increase of the hydrogen-bond basicity of the IL increases their ability to wet polar surfaces whereas it reduces their capability to wet non-polar ones.

In order to further develop predictive correlations for the contact angles of ILs, the set of experimental data here obtained was correlated with cation-anion interaction energies generated using COSMO-RS, a quantum chemical-based prediction model. The high correlation coefficients and Fisher significance parameters obtained validated the *a priori* cation-anion interaction energy descriptors for the prediction of the ILs contact angles. Accordingly, two-descriptor correlations were proposed to predict the contact angles of ILs on the polar glass and Al-plate surfaces as well as in the non-polar PTFE surface. These correlations may be valuable for the design and applications of a target IL with pre-defined wettability. A final databank comprising the contact angles of 480 ILs in 3 surfaces was here proposed.

## Materials and Methods

### Materials

A broad range of ILs was studied in this work in order to evaluate the impact of their chemical structures, namely the cation core, the anion nature, and the cation alkyl side chain length, on the contact angles of ILs in both polar and non-polar surfaces. The ILs investigated were: 1-butyl-3-methylimidazolium acetate, [C<sub>4</sub>C<sub>1</sub>im][Ac]; 1-butyl-3-methylimidazolium dimethylphosphate, [C<sub>4</sub>C<sub>1</sub>im][DMP]; 1-butyl-3-methylimidazolium trifluoroacetate, [C<sub>4</sub>C<sub>1</sub>im][TFA]; 1-butyl-3-methylimidazolium dicyanamide, [C<sub>4</sub>C<sub>1</sub>im][N(CN)<sub>2</sub>]; 1-butyl-3-methylimidazolium ethylsulphate, [C<sub>4</sub>C<sub>1</sub>im][EtSO<sub>4</sub>]; 1-butyl-3-methylimidazolium methylsulphate, [C<sub>4</sub>C<sub>1</sub>im][MeSO<sub>4</sub>]; 1-butyl-3-methylimidazolium trifluoromethanesulfonate, [C<sub>4</sub>C<sub>1</sub>im][CF<sub>3</sub>SO<sub>3</sub>]; 1-butyl-3-methylimidazolium thiocyanate, [C<sub>4</sub>C<sub>1</sub>im][SCN]; 1-butyl-3-methylimidazolium tricyanomethane, [C<sub>4</sub>C<sub>1</sub>im][C(CN)<sub>3</sub>]; 1-butyl-3-methylimidazolium tetrafluoroborate, [C<sub>4</sub>C<sub>1</sub>im][BF<sub>4</sub>]; 1-butyl-3-methylimidazolium hexafluorophosphate, [C<sub>4</sub>C<sub>1</sub>im][PF<sub>6</sub>]; 1-butyl-3-methylimidazolium bis(trifluoromethylsulfonyl)imide, [C<sub>4</sub>C<sub>1</sub>im][NTf<sub>2</sub>]; 1-ethyl-3-methylimidazolium bis(trifluoromethylsulfonyl)imide, [C<sub>2</sub>C<sub>1</sub>im][NTf<sub>2</sub>]; 1-methyl-3-propylimidazolium bis(trifluoromethylsulfonyl)imide, [C<sub>3</sub>C<sub>1</sub>im][NTf<sub>2</sub>]; 1-methyl-3-pentylimidazolium bis(trifluoromethylsulfonyl)imide, [C<sub>5</sub>C<sub>1</sub>im][NTf<sub>2</sub>]; 1-hexyl-3-methylimidazolium bis(trifluoromethylsulfonyl)imide, [C<sub>6</sub>C<sub>1</sub>im][NTf<sub>2</sub>]; 1-heptyl-3-methylimidazolium bis(trifluoromethylsulfonyl)imide, [C<sub>7</sub>C<sub>1</sub>im][NTf<sub>2</sub>]; 1-methyl-3-octylimidazolium bis(trifluoromethylsulfonyl)imide, [C<sub>8</sub>C<sub>1</sub>im][NTf<sub>2</sub>]; 1-methyl-3-nonylimidazolium bis(trifluoromethylsulfonyl)imide, [C<sub>9</sub>C<sub>1</sub>im][NTf<sub>2</sub>]; 1-methyl-1-propylpiperidinium bis(trifluoromethylsulfonyl)imide, [C<sub>3</sub>C<sub>1</sub>pip][NTf<sub>2</sub>]; 1-butyl-1-

methylpiperidinium bis(trifluoromethylsulfonyl)imide,  $[\text{C}_4\text{C}_1\text{pip}][\text{NTf}_2]$ ; and 1-butyl-4-methylpyridinium bis(trifluoromethylsulfonyl)imide,  $[\text{C}_4\text{-4-C}_1\text{im}][\text{NTf}_2]$ . The chemical structures of the ions of the ILs investigated are given in Figure 3. These ILs were purchased from Iolitec with a purity level higher than 98 wt%. Prior to the measurements of contact angles, individual samples of each IL were dried under constant agitation and vacuum ( $10^{-2}$  Pa) at 323 K for at least 48 h in order to remove traces of water and volatile compounds.

After this procedure, the purity of each IL was further checked using  $^1\text{H}$ ,  $^{13}\text{C}$ , and  $^{19}\text{F}$  (whenever possible) NMR spectroscopy.

The solid substrates studied were poly-(tetrafluoroethylene) (PTFE) with 1 mm thickness (Goodfellow), Al-plate (Extrusal) and optical quality glass (VWR). The substrates were carefully cleaned with a detergent solution, rinsed several times with distilled and deionized water, dried with nitrogen and for 2 h inside a vacuum oven at room temperature.

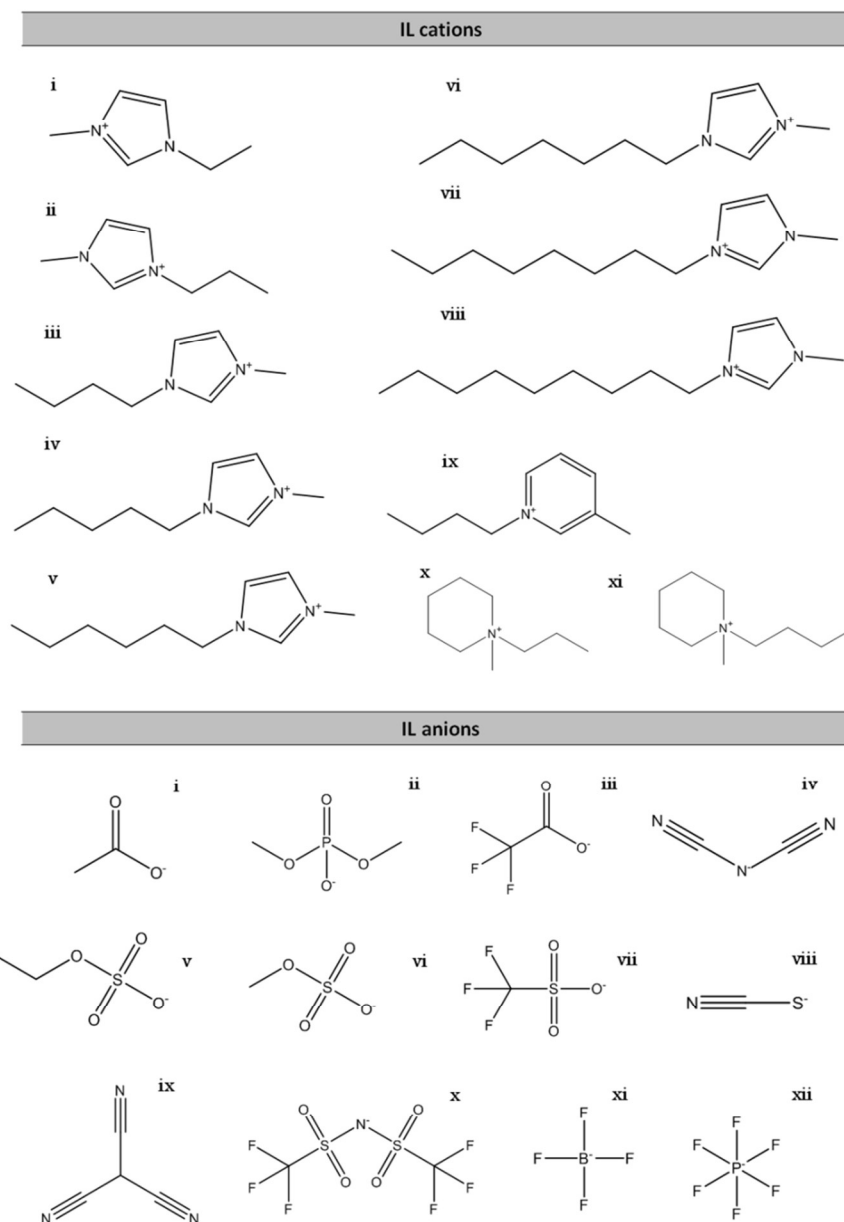


Figure 3. Chemical structures of cations and anions composing the studied ILs. Cations: (i) 1-ethyl-3-methylimidazolium (ii) 1-propyl-3-methylimidazolium, (iii) 1-butyl-3-methylimidazolium, (iv) 1-pentyl-3-methylimidazolium, (v) 1-hexyl-3-methylimidazolium, (vi) 1-heptyl-3-methylimidazolium, (vii) 1-octyl-3-methylimidazolium, (viii) 1-nonyl-3-methylimidazolium, (ix) 1-butyl-3-methylpyridinium, (x) 1-methyl-1-propylpyridinium, and (xi) 1-butyl-1-methylpiperidinium. Anions: (i) acetate, (ii) dimethylphosphate, (iii) trifluoroacetate, (iv) dicyanamide, (v) ethylsulfate, (vi) methylsulfate, (vii) trifluoromethanesulfonate, (viii) thiocyanate, (ix) tricyanomethane (x) bis(trifluoromethylsulfonyl)imide, (xi) tetrafluoroborate, and (xii) hexafluorophosphate.

## Contact Angle Measurements

Contact angle measurements were carried out using the sessile drop method with the Contact Angle System OCA 20 (DataPhysics Instruments GmbH, Germany) at 298.2 K. Drop volumes of  $(2 \pm 0.01) \mu\text{L}$  were obtained using a Hamilton DS 500/GT syringe connected to a Teflon coated needle placed inside an aluminium chamber able to maintain the temperature of interest within  $\pm 0.1$  K. The contact angle evolution over time was recorded, for time intervals ranging from 10 to 60 min, depending on the liquid spreading kinetics. When a plateau was achieved, the so-called static contact angle was recorded. The reported contact angles of each IL are an average of at least five independent measurements.

## COSMO-RS Calculations

The Conductor-like Screening Model for Real Solvents (COSMO-RS), developed by Klamt and co-workers,<sup>33,34</sup> is a quantum chemical based method used for the prediction of the thermodynamic properties of pure and mixed fluids. In COSMO-RS, molecules are treated as a collection of surface segments. An expression for the chemical potential of segments in the condensed phase is derived, and in which the interaction energies between segments are calculated from COSMO-RS. The chemical potential of each molecule is then obtained by summing the contributions of the segments. The advantage of using COSMO-RS compared to other prediction methods, such as Quantitative Structure-Properties Relationship (QSPR), is that this model only requires the chemical structures information of the desired molecules and thus, can be simply used as *a priori* approach. In addition, owing to its quantum chemical-based approach, it provides a more accurate and detailed description of the electronic/molecular descriptors than empirical methods.<sup>48</sup>

In this work, the cation-anion pair interaction energies were generated using the COSMOthermX program, parameter file BP\_TZVP\_C20\_0111 (COSMOlogic GmbH & Co KG, Leverkusen, Germany).<sup>49</sup> All the COSMO files required are available in the COSMOthermX database. In COSMO-RS, the total IL cation-anion interaction energy ( $E_{\text{INT}}$ ) arises from the sum of three specific interactions, namely electrostatic-misfit ( $E_{\text{MF}}$ ), hydrogen-bond ( $E_{\text{HB}}$ ), and van der Waals forces ( $E_{\text{vdW}}$ ) that can be expressed as

$$E_{\text{INT}} = E_{\text{MF}} + E_{\text{HB}} + E_{\text{vdW}} \quad (7)$$

In addition to those four descriptors, we introduced an additional descriptor, namely the ring correction energy,  $E_{\text{Ring}}$ , which depends on the number of atoms which compose a given IL cation ring (see Table S1 in the ESI†).

In a previous work,<sup>28</sup> the best predictions of the experimental data were obtained with the lowest energy conformations or with the global minimum for both the IL cation and anion. Thus, in this work, the lowest energy conformations of all species involved were used in the COSMO-RS calculations.

## Acknowledgments

This work was developed in the scope of project CICECO – Aveiro Institute of Materials (Ref. FCT UID/CTM/50011/2013), financed by national funds through Fundação para a Ciência e a Tecnologia (FCT, Portugal)/MEC and co-financed by FEDER under the PT2020 Partnership agreement. Thanks are also due to FCT/MEC for the financial support to the QOPNA research Unit (FCT UID/QUI/00062/2013), through national funds, co-financed by FEDER within the PT2020 Partnership Agreement. M.M. Pereira and F.L. Sousa acknowledge the financial support from Coordenação de Aperfeiçoamento de Pessoal de Nível Superior - Capes for the PhD grant (2740-13-3) and FCT for the post-doctoral grant SFRH/BPD/71033/2010, respectively. M.G. Freire acknowledges the European Research Council (ERC) for the Grant ERC-2013-StG-337753.

## Notes and references

<sup>a</sup>CICECO - Aveiro Institute of Materials, Department of Chemistry, University of Aveiro, 3810-193 Aveiro, Portugal. E-mail address: maragfreire@ua.pt; Tel: +351-234-401422; Fax: +351-234-370084

<sup>b</sup>Center of Research in Ionic Liquids, Department of Chemical Engineering, Universiti Teknologi PETRONAS, Bandar Seri Iskandar 32610 Perak, Malaysia

<sup>c</sup>CICECO - Aveiro Institute of Materials, Departamento de Física, Universidade de Aveiro, 3810-193 Aveiro, Portugal

<sup>d</sup>QOPNA Unit, Department of Chemistry, Universidade de Aveiro, 3810-193 Aveiro, Portugal

<sup>e</sup>Equally contributing authors

†Electronic Supplementary Information (ESI) available: [Comparison between experimental and prediction of contact angles of ILs on polar and non-polar surfaces; IL cation-anion interaction energies predicted using COSMO-RS; Multi parameter sets for the correlations of contact angles and IL cation-anion interaction energies; Full name, abbreviation, and numbering of ILs; and predicted contact angles for 480 ILs on both polar and non-polar surfaces]. See DOI: 10.1039/b000000x/

## References

- Wasserscheid, P.; Welton, T. *Ionic Liquids in Synthesis*; 2nd ed. ed.; WILEY-VCH Verlag GmbH & Co. KGaA: Darmstadt, Federal Republic of Germany, 2009; Vol. Vol. 1.
- Rogers, R. D. *Nature* 2007, **447**, 917.
- Plechkova, N. V.; Seddon, K. R. *Chem. Soc. Rev.* 2008, **37**, 123.
- An, Y.; Cheng, X.; Zuo, P.; Liao, L.; Yin, G. *Mater. Chem. Phys* 2011, **128**, 250.
- Bazito, F. F. C.; Kawano, Y.; Torresi, R. M. *Electrochim. Acta* 2007, **52**, 6427.
- Tariq, M.; Freire, M. G.; Saramago, B.; Coutinho, J. A. P.; Lopes, J. N. C.; Rebelo, L. P. N. *Chem. Soc. Rev.* 2012, **41**, 829.
- Page, P. M.; McCarty, T. A.; Baker, G. A.; Baker, S. N.; Bright, F. V. *Langmuir* 2007, **23**, 843.
- Gao, L.; McCarthy, T. J. *J. Am. Chem. Soc* 2007, **129**, 3804.
- Restolho, J.; Mata, J. L.; Saramago, B. *J. Colloid Interface Sci* 2009, **340**, 82.
- Restolho, J.; Mata, J. L.; Saramago, B. *J. Chem. Phys.* 2011, **134**.

- 11 Restolho, J.; Mata, J. L.; Saramago, B. *Fluid Phase Equilib.* 2012, **322–323**, 142.
- 12 Restolho, J.; Mata, J. L.; Shimizu, K.; Canongia Lopes, J. N.; Saramago, B. *J. Phys. Chem. C* 2011, **115**, 16116.
- 13 Carrera, G. V. S. M.; Afonso, C. A. M.; Branco, L. C. *J. Chem. Eng. Data* 2010, **55**, 609.
- 14 Paneru, M.; Priest, C.; Sedev, R.; Ralston, J. *J. Phys. Chem. C* 2010, **114**, 8383.
- 15 Millefiorini, S.; Tkaczyk, A. H.; Sedev, R.; Efthimiadis, J.; Ralston, J. *J. Am. Chem. Soc.* 2006, **128**, 3098.
- 16 Paneru, M.; Priest, C.; Ralston, J.; Sedev, R. *J. Adhes. Sci. Technol.* 2012, **26**, 2047.
- 17 Halka, V.; Freyland, W. *Zeitschrift fur Physikalische Chemie* 2008, **222**, 117.
- 18 Restolho, J.; Mata, J. L.; Saramago, B. *J. Phys. Chem. C* 2009, **113**, 9321.
- 19 Freire, M. G.; Neves, C. M. S. S.; Carvalho, P. J.; Gardas, R. L.; Fernandes, A. M.; Marrucho, I. M.; Santos, L. M. N. B. F.; Coutinho, J. A. P. *J. Phys. Chem. B* 2007, **111**, 13082.
- 20 Freire, M. G.; Carvalho, P. J.; Gardas, R. L.; Santos, L. M. N. B. F.; Marrucho, I. M.; Coutinho, J. A. P. *J. Chem. Eng. Data* 2008, **53**, 2378.
- 21 Kurnia, K. A.; Sintra, T. E.; Neves, C. M. S. S.; Shimizu, K.; Canongia Lopes, J. N.; Goncalves, F.; Ventura, S. P. M.; Freire, M. G.; Santos, L. M. N. B. F.; Coutinho, J. A. P. *Phys. Chem. Chem. Phys.* 2014, **16**, 19952.
- 22 Kurnia, K. A.; Quental, M. V.; Santos, L. B.; Freire, M. G.; Coutinho, J. A. P. *Phys. Chem. Chem. Phys.* 2015, **17**, 4569.
- 23 Freire, M. G.; Carvalho, P. J.; Gardas, R. L.; Marrucho, I. M.; Santos, L. M. N. B. F.; Coutinho, J. A. P. *J. Phys. Chem. B* 2008, **112**, 1604.
- 24 Freire, M. G.; Neves, C. M. S. S.; Shimizu, K.; Bernardes, C. E. S.; Marrucho, I. M.; Coutinho, J. A. P.; Canongia Lopes, J. N.; Rebelo, L. P. N. *J. Phys. Chem. B* 2010, **114**, 15925.
- 25 Martins, M. A. R.; Neves, C. M. S. S.; Kurnia, K. A.; Andreia, L.; Santos, L. M. N. B. F.; Freire, M. G.; Pinho, S. P.; Coutinho, J. A. P. *Fluid Phase Equilib.* 2014, **375**, 161.
- 26 Neves, C. M. S. S.; Kurnia, K. A.; Shimizu, K.; Marrucho, I. M.; Rebelo, L. P. N.; Coutinho, J. A. P.; Freire, M. G.; Canongia Lopes, J. N. *Phys. Chem. Chem. Phys.* 2014, **16**, 21340.
- 27 Martins, M. A. R.; Neves, C. M. S. S.; Kurnia, K. A.; Santos, L. M. N. B. F.; Freire, M. G.; Pinho, S. P.; Coutinho, J. A. P. *Fluid Phase Equilib.* 2014, **381**, 28.
- 28 Cláudio, A. F. M.; Swift, L.; Hallett, J. P.; Welton, T.; Coutinho, J. A. P.; Freire, M. G. *Phys. Chem. Chem. Phys.* 2014, **16**, 6593.
- 29 Kurnia, K. A.; Lima, F.; Cláudio, A. F. M.; Coutinho, J. A. P.; Freire, M. G. *Phys. Chem. Chem. Phys.* 2015, **17**, 18980.
- 30 Kurnia, K. A.; Pinho, S. P.; Coutinho, J. A. P. *Green Chem.* 2014, **16**, 3741.
- 31 Ferreira, A. R.; Freire, M. G.; Ribeiro, J. C.; Lopes, F. M.; Crespo, J. G.; Coutinho, J. A. P. *Fuel* 2014, **128**, 314.
- 32 Neves, C. M. S. S.; Granjo, J. F. O.; Freire, M. G.; Robertson, A.; Oliveira, N. M. C.; Coutinho, J. A. P. *Green Chem.* 2011, **13**, 1517.
- 33 Klamt, A.; Eckert, F. *Fluid Phase Equilib.* 2000, **172**, 43.
- 34 Klamt, A. *COSMO-RS from quantum chemistry to fluid phase thermodynamics and drug design*; Elsevier: Amsterdam, The Netherlands, 2005.
- 35 Batchelor, T.; Cunder, J.; Fadeev, A. Y. *J. Colloid Interface Sci* 2009, **330**, 415.
- 36 Freire, M. G.; Neves, C. M. S. S.; Marrucho, I. M.; Coutinho, J. A. P.; Fernandes, A. M. *J. Phys. Chem. A* 2010, **114**, 3744.
- 37 Cione, A. M.; Mazyar, O. A.; Booth, B. D.; McCabe, C.; Jennings, G. K. *J. Phys. Chem. C* 2009, **113**, 2384.
- 38 Ferreira, R.; Blesic, M.; Trindade, J.; Marrucho, I.; Lopes, J. N. C.; Rebelo, L. P. N. *Green Chem.* 2008, **10**, 918.
- 39 Anwander, R.; Palm, C.; Groeger, O.; Engelhardt, G. *Organometallics* 1998, **17**, 2027.
- 40 Li, H.; Sedev, R.; Ralston, J. *Phys. Chem. Chem. Phys.* 2011, **13**, 3952.
- 41 Lemus, J.; Neves, C. M. S. S.; Marques, C. F. C.; Freire, M. G.; Coutinho, J. A. P.; Palomar, J. *Environmental Sciences: Processes and Impacts* 2013, **15**, 1752.
- 42 Lemus, J.; Martin-Martinez, M.; Palomar, J.; Gomez-Sainero, L.; Gilarranz, M. A.; Rodriguez, J. J. *Chem. Eng. J.* 2012, **211–212**, 246.
- 43 Neves, C. M. S. S.; Lemus, J.; Freire, M. G.; Palomar, J.; Coutinho, J. A. P. *Chem. Eng. J.* 2014, **252**, 305.
- 44 Ab Rani, M. A.; Brant, A.; Crowhurst, L.; Dolan, A.; Lui, M.; Hassan, N. H.; Hallett, J. P.; Hunt, P. A.; Niedermeyer, H.; Perez-Arlandis, J. M.; Schrems, M.; Welton, T.; Wilding, R. *Phys. Chem. Chem. Phys.* 2011, **13**, 16831.
- 45 Palomar, J.; Ferro, V. R.; Torrecilla, J. S.; Rodríguez, F. *Ind. Eng. Chem. Res.* 2007, **46**, 6041.
- 46 Palomar, J.; Torrecilla, J. S.; Lemus, J.; Ferro, V. R.; Rodriguez, F. *Phys. Chem. Chem. Phys.* 2010, **12**, 1991.
- 47 Ghanem, O. B.; Mutalib, M.; El-Harbawi, M.; Gonfa, G.; Kait, C. F.; Alitheen, N. B. M.; Lévêque, J. M. *J. Hazard. Mater* 2015, **297**, 198.
- 48 Karelson, M.; Lobanov, V. S.; Katritzky, A. R. *Chem. Rev* 1996, **96**, 1027.
- 49 Eckert, F.; Klamt, A.; COSMOlogic GmbH & Co. KG, Leverkusen, Germany: 2006.